

Quench Spectroscopy for Dissipative and Non-Hermitian Quantum Lattice Models

Julien Despres^{1,*}

1 JEIP, USR 3573 CNRS, Collège de France, PSL Research University, 11 Place Marcelin Berthelot, 75321 Paris Cedex 05, France

* jdespres@planckian.co

Abstract

We study the dynamics of the open Bose-Hubbard chain confined in the superfluid phase submitted to a sudden global quench on the dissipations and the repulsive interactions. The latter is investigated by calculating the equations of motion of relevant quadratic correlators permitting to study the equal-time connected one-body and density-density correlations functions. We then compute the quench spectral function associated to each observable to perform the quench spectroscopy of this dissipative quantum lattice model. This permits to unveil the quasiparticle dispersion relation of the Bose-Hubbard chain in the superfluid phase in the presence of loss processes. The applicability of the quench spectroscopy is also generalized to non-Hermitian quantum lattice models by considering the non-Hermitian transverse-field Ising chain in the paramagnetic phase.

Contents

1	Introduction	1
2	Model and quench procedure	3
3	Quench dynamics of the isolated Bose-Hubbard chain	5
4	Double quench dynamics of the Bose-Hubbard chain	9
5	Quench spectroscopy of the double-quenched Bose-Hubbard chain	10
6	Experimental feasibility of the quench spectroscopy method	12
7	Applicability of the quench spectroscopy to a non-Hermitian quantum lattice model	14
8	Conclusion	16
	References	16

1 Introduction

In the last decades, the major progress in the experimental control of quantum lattice models has given consequent momentum to the analytical and experimental investigation of the quench dynamics of isolated quantum systems [1–6]. Recently, a new spectroscopy method has been introduced theoretically and verified numerically using tensor networks for isolated quantum spin and bosonic lattice models. The latter is based on the dynamical properties of the model induced by weak sudden global or local quenches [7, 8] and is referred to as quench spectroscopy. This new method to determine low-lying excitation spectra has been recently applied experimentally to the dipolar XY model using Rydberg atoms [9] and has provided promising results. However, since quantum systems cannot be

purely isolated from their environment, it is natural that the study of open quantum systems has attracted a lot of interest in the last few years [10–12] by taking into account dissipative effects such as local dephasing noise [13–17], incoherent hopping [18] and local gain/loss processes [19–27]. These open quantum lattice models are governed by the well-known Lindblad master equation [28–31] characterising the time evolution of the quantum system density matrix. However, the possibility to apply the quench spectroscopy for open quantum lattice models has not been investigated and corresponds to the main study of the present research work.

Experimentally, quantum simulators based on trapped ultracold atoms loaded in an artificial optical lattice generated by the interference of counter-propagating laser beams permit to simulate quantum lattice models [32, 33]. Using bosonic atoms, the Bose-Hubbard model can thus be engineered [34, 35]. Its out-of-equilibrium properties are accessible via quantum quenches realised experimentally by suddenly modifying the intensity of the laser beams controlling the artificial lattice depth and thus the ratio between the hopping amplitude and the two-body repulsive interaction strength [3, 36]. This tuning of the interaction ratio offers the possibility to scan the quantum phase transition between the gapless superfluid and Mott-insulating phases for commensurate fillings of the lattice. Loss processes, inducing a rich and new physics such as the quantum Zeno effect [37], the loss-assisted quantum control [38] or the loss-induced cooling effect [39], can be generated using this experimental platform based on ultracold bosonic atoms where different number of particles can be involved. For instance, two-body losses can be engineered by light-assisted inelastic two-body collisions which can also occur naturally in ultracold-atom experiments [21, 40–44].

In this work, we propose to investigate the dynamics of the open Bose-Hubbard chain driven out of equilibrium via sudden global quenches on the interactions as well as on the dissipations. The dissipative effects consist here in on-site two-body losses. The term *on-site* refers to a loss process involving a single lattice site. This specific quantum lattice model as well as its quench dynamics can be simulated experimentally using ultracold bosonic atoms [3, 45–47] including a controllable strength of the on-site two-body losses engineered by light-assisted inelastic collisions [21, 42–44]. The quench dynamics of the isolated Bose-Hubbard chain has already been extensively studied theoretically and numerically using for instance tensor network or variational Monte-Carlo techniques [7, 8, 48–58]. Regarding the latter in the presence of dissipations, its quench dynamics induced by two-body losses has been under-researched analytically and numerically [59–61]. Most importantly, the possibility to perform quench spectroscopy to dissipative quantum lattice models has not been studied. The latter statement is also valid for non-Hermitian quantum lattice models. These exotic class of quantum systems appear naturally when studying the dynamics of dissipative quantum lattice models in the so-called no-click limit [31]. Consequently, we also propose here to investigate the quench spectroscopy of the non-Hermitian ($s = 1/2$ short-range interacting) transverse-field Ising chain confined in its paramagnetic phase. This underlines the importance of the research work presented here together with the possibility to confirm our conclusions experimentally at least for generic dissipative quantum lattice models.

We first introduce the theoretical approach based on the calculation of the equations of motion associated to the relevant quadratic bosonic correlators. The latter is valid in the superfluid-mean-field regime of the Bose-Hubbard chain for on-site two-body losses. The latter is benchmarked with a quasiparticle theory for the isolated Bose-Hubbard chain for a sudden global quench on the repulsive interactions. The former theory is adapted to investigate the double quench dynamics of the Bose-Hubbard chain where both the interactions and the dissipations are quenched suddenly and globally. This will permit to investigate the quench spectroscopy of the dissipative Bose-Hubbard chain. We then discuss the applicability of the quench spectroscopy method to non-Hermitian quantum lattice models by considering the quench dynamics of the non-Hermitian transverse-field Ising chain confined in the (paramagnetic) z polarized phase.

This article is organised as follows: in Sec 2, we start by introducing the model and the quench procedure. In Sec. 3, we benchmark the equations of motion approach with a quasiparticle approach. In Sec. 4, we discuss the dissipative and interaction quench dynamics of the Bose-Hubbard chain for on-site two-body losses. In Sec. 5, we investigate theoretically the quench spectroscopy of the latter dissipative quantum lattice model. In Sec. 6, we discuss the experimental feasibility as well as the limitations associated to the quench spectroscopy method. Then, in Sec. 7, the quench spectroscopy approach is extended to non-Hermitian quantum lattice models by applying the latter to the non-Hermitian transverse-field Ising chain confined in its paramagnetic phase. Finally in Sec. 8, we present our conclusions and possible extensions of the presented research work.

2 Model and quench procedure

We focus on the one-dimensional Bose-Hubbard (1D BH) model for a lattice chain of length L whose lattice spacing is fixed to unity, i.e. $a = 1$, with periodic boundary conditions; for simplicity, we also set $\hbar = 1$. The corresponding Hamiltonian \hat{H} reads:

$$\hat{H} = -J \sum_R (\hat{b}_R^\dagger \hat{b}_{R+1} + \text{h.c.}) + \frac{U}{2} \sum_R \hat{n}_R (\hat{n}_R - 1), \quad (1)$$

where \hat{b}_R and \hat{b}_R^\dagger correspond to the bosonic annihilation and creation operators acting on the lattice site $R \in \mathbb{N}$, $\hat{n}_R = \hat{b}_R^\dagger \hat{b}_R$ denotes the local occupation number operator associated to the lattice site index R , $J > 0$ corresponds to the hopping amplitude, $U > 0$ is the on-site repulsive two-body interaction strength. At equilibrium and zero-temperature, the quantum phase diagram of the BH chain has been extensively studied [62, 63]. The latter displays a gapless superfluid (SF) phase and a gapped Mott-insulating (MI) phase with the so-called Mott lobes, determined by the competition between the hopping, the interactions and the chemical potential μ or equivalently the average filling \bar{n} depending if the grand canonical or canonical ensemble is considered. In what follows, we rely on the average filling where for $\bar{n} \in \mathbb{N}^*$, the SF-MI phase transition is of the Berezinskii-Kosterlitz-Thouless type at the critical value $(U/J)_c \simeq 3.3$ for $\bar{n} = 1$ [64–67]. For non-integer fillings, the quantum system remains in the SF phase for any value of the dimensionless interaction parameter U/J .

The dissipative quench dynamics associated to the BH chain is fully characterised by the Lindblad master equation which reads as:

$$\frac{d}{dt} \hat{\rho}(t) = -i [\hat{H}, \hat{\rho}(t)] + \sum_R \hat{L}_R \hat{\rho}(t) \hat{L}_R^\dagger - \frac{1}{2} \{ \hat{L}_R^\dagger \hat{L}_R, \hat{\rho}(t) \}, \quad (2)$$

where \hat{H} refers to the Hamiltonian of the BH chain defined at Eq. (1). $\hat{\rho}(t)$ refers to the time-dependent density matrix and \hat{L}_R to the Lindblad jump operator acting on the lattice site R . For on-site two-body losses, $\hat{L}_R = \sqrt{\gamma} \hat{b}_R^2$ where γ corresponds to the dissipation strength also called dissipation rate.

To drive the BH chain out of equilibrium, the following quench procedure is considered. We start from an initial many-body quantum state corresponding to the ground state of the 1D BH model without dissipation implying $\gamma = 0$. Initially, the density or equivalently the filling since $a = 1$ is unitary, i.e. $\bar{n} = 1$. Then, we let the quantum lattice model evolve with a non-zero value of the dissipation strength $\gamma > 0$. The latter defines the first quench corresponding to an dissipation quench. The second one is performed on the dimensionless interaction parameter U/J hence corresponding to an interaction quench. It is done by considering a pre-quench value U_i/J quenched to a post-quench value U_f/J . Note that the hopping amplitude J is fixed during the full real time evolution. The double quench dynamics is studied starting from a many-body ground state of the BH chain confined in the SF phase, i.e. $U/J < (U/J)_c$. To characterise the system's dynamics, we investigate a variety of quantum observables including $G_1(R, t) = \langle \hat{b}_R^\dagger(t) \hat{b}_0(t) \rangle_c$ the connected one-body correlation function and $G_2(R, t) = \langle \hat{n}_R(t) \hat{n}_0(t) \rangle_c$ the connected density-density correlation function. The phase and density fluctuations determined by G_1 and G_2 can be measured in ultracold-atom experiments using time-of-flight and fluorescence microscopy imaging respectively [3, 36, 46, 47].

To investigate theoretically the dissipative quench dynamics induced by on-site two-body losses of the BH chain initially confined in the SF-mean-field regime, we relied on an analytical result from the scientific publication of *J.Despres et al.* at Ref. [59]. In the latter paper, the set of equations of motion (EoMs) associated to the correlators $G_k(t) = \langle \hat{b}_k^\dagger \hat{b}_k \rangle_t$ and $F_k(t) = \langle \hat{b}_{-k} \hat{b}_k \rangle_t$ for the BH model on a D -dimensional hypercubic lattice for long-range two-body losses has been calculated. Using the Lindblad master equation, the EoMs are given by:

$$\frac{d}{dt} G_k(t) = i \langle [\hat{H}(t), \hat{n}_k] \rangle_t + \frac{1}{2} \sum_{R,R'} \left(\langle \hat{L}_{R,R'}^\dagger [\hat{n}_k, \hat{L}_{R,R'}] \rangle_t + \text{h.c.} \right); \quad (3a)$$

$$\frac{d}{dt} F_k(t) = i \langle [\hat{H}(t), \hat{b}_{-k} \hat{b}_k] \rangle_t + \sum_{R,R'} \langle \hat{L}_{R,R'}^\dagger \hat{b}_{-k} \hat{b}_k \hat{L}_{R,R'} \rangle_t - \frac{1}{2} \langle \hat{b}_{-k} \hat{b}_k \hat{L}_{R,R'}^\dagger \hat{L}_{R,R'} \rangle_t - \frac{1}{2} \langle \hat{L}_{R,R'}^\dagger \hat{L}_{R,R'} \hat{b}_{-k} \hat{b}_k \rangle_t, \quad (3b)$$

where $\hat{H}(t)$ denotes the quadratic form in Fourier space of the BH model in the SF-mean-field regime with a time-dependent filling $\bar{n}(t)$ or equivalently a time-dependent density $n(t)$. \hat{b}_k and \hat{b}_k^\dagger correspond to the bosonic annihilation and creation operators acting in the reciprocal space on the momentum \mathbf{k} ; $\hat{n}_k = \hat{b}_k^\dagger \hat{b}_k$ denotes the occupation

number operator in Fourier space for the momentum \mathbf{k} . The previous set of equations is characterized by the Lindblad jump operator $\hat{L}_{\mathbf{R},\mathbf{R}'}$ as well as the long-range dissipation strength $\gamma_{\|\mathbf{R}-\mathbf{R}'\|}$ which read as:

$$\hat{L}_{\mathbf{R},\mathbf{R}'} = \sqrt{\gamma_{\|\mathbf{R}-\mathbf{R}'\|}} \hat{b}_{\mathbf{R}} \hat{b}_{\mathbf{R}'}, \quad \gamma_{\|\mathbf{R}-\mathbf{R}'\|} = \frac{\Gamma}{(1 + \|\mathbf{R}-\mathbf{R}'\|)^\alpha}, \quad (4)$$

with $\|\cdot\|$ standing for the vector norm and α for the power-law exponent characterizing the spatial decay of the long-range two-body loss processes. The Hermiticity of the occupation number operator in momentum space $\hat{n}_{\mathbf{k}}$ has been considered to simplify the EoM associated to the correlator $G_{\mathbf{k}}(t)$. To calculate the EoMs while considering the SF-mean-field regime, a decoupling of the condensate mode $\mathbf{k} = \mathbf{0}$ from the other modes is used together with a mean-field approximation where only the terms depending on correlators involving four or two bosonic operators acting on the mode $\mathbf{k} = \mathbf{0}$ are conserved. As a consequence, the EoMs associated to $G_{\mathbf{k}}(t)$ and $F_{\mathbf{k}}(t)$ both for $\mathbf{k} = \mathbf{0}$ and $\mathbf{k} \neq \mathbf{0}$ have been calculated. Finally, the following set of EoMs is found:

$$\frac{d}{dt} G_0(t) = - \sum_{\mathbf{q} \neq \mathbf{0}} [(\mathcal{G}_{\mathbf{q}} + \mathcal{H}_{\mathbf{q}}) F_0(t) F_{\mathbf{q}}(t)^* + \text{h.c.}] - \sum_{\mathbf{q} \neq \mathbf{0}} \mathcal{F}_{\mathbf{q}} G_0(t) G_{\mathbf{q}}(t) - 2\mathcal{G}_0 G_0(t) (G_0(t) - 1); \quad (5a)$$

$$\frac{d}{dt} F_0(t) = -\mathcal{G}_0 (2G_0(t) - 3) F_0(t) - \sum_{\mathbf{q} \neq \mathbf{0}} \mathcal{F}_{\mathbf{q}} F_0(t) G_{\mathbf{q}}(t) - \sum_{\mathbf{q} \neq \mathbf{0}} (\mathcal{G}_{\mathbf{q}} + \mathcal{H}_{\mathbf{q}}) (2G_0(t) + 1) F_{\mathbf{q}}(t); \quad (5b)$$

$$\frac{d}{dt} G_{\mathbf{k}}(t) = -2\mathcal{B}_{\mathbf{k}}(t) \text{Im}(F_{\mathbf{k}}(t)) - \mathcal{G}_{\mathbf{k}} (F_0(t) F_{\mathbf{k}}(t)^* + \text{h.c.}) - \mathcal{F}_{\mathbf{k}} G_0(t) G_{\mathbf{k}}(t) \quad \forall \mathbf{k} \neq \mathbf{0}; \quad (5c)$$

$$\frac{d}{dt} F_{\mathbf{k}}(t) = -[2i\mathcal{A}_{\mathbf{k}}(t) + \mathcal{F}_{\mathbf{k}} G_0(t)] F_{\mathbf{k}}(t) - [i\mathcal{B}_{\mathbf{k}}(t) + \mathcal{G}_{\mathbf{k}} F_0(t)] (2G_{\mathbf{k}}(t) + 1) \quad \forall \mathbf{k} \neq \mathbf{0}, \quad (5d)$$

where the momentum- (and possibly time-) dependent functions $\mathcal{A}_{\mathbf{k}}(t)$, $\mathcal{B}_{\mathbf{k}}(t)$, $\mathcal{F}_{\mathbf{q}}$, $\mathcal{G}_{\mathbf{q}}$ and $\mathcal{H}_{\mathbf{q}}$ are defined as follows:

$$\mathcal{A}_{\mathbf{k}}(t) = 4J \sum_{i=1}^D \sin^2\left(\frac{\mathbf{k} \cdot \mathbf{d}_i}{2}\right) + \mathcal{B}_{\mathbf{k}}(t); \quad (6)$$

$$\mathcal{B}_{\mathbf{k}}(t) = \frac{U}{L^D} \sum_{\mathbf{q}} G_{\mathbf{q}}(t) = U\bar{n}(t); \quad (7)$$

$$\mathcal{F}_{\mathbf{q}} = 2(\mathcal{G}_0 + \mathcal{G}_{\mathbf{q}}); \quad (8)$$

$$\mathcal{G}_{\mathbf{q}} = \frac{1}{L^{2D}} \sum_{\mathbf{R},\mathbf{R}'} \gamma_{\|\mathbf{R}-\mathbf{R}'\|} \cos(\mathbf{q} \cdot (\mathbf{R} - \mathbf{R}')); \quad (9)$$

$$\mathcal{H}_{\mathbf{q}} = \frac{1}{L^{2D}} \sum_{\mathbf{R},\mathbf{R}'} \gamma_{\|\mathbf{R}-\mathbf{R}'\|} i \sin(\mathbf{q} \cdot (\mathbf{R} - \mathbf{R}')), \quad (10)$$

with $\mathbf{k} = (k_x, k_y, k_z, \dots)^T$, $\mathbf{d}_i = (0, \dots, 0, a_i, 0, \dots, 0)^T$ with $a_i = 1$ denoting the lattice spacing along the i -th spatial dimension and $i \in [1, D]$. For our case study corresponding to the BH model on a 1D lattice chain, i.e. $D = 1$, while considering on-site two-body losses, i.e. $\alpha \rightarrow +\infty$ leading to $\gamma_{\mathbf{R}-\mathbf{R}'} = \Gamma \delta_{\mathbf{R},\mathbf{R}'} = \gamma \delta_{\mathbf{R},\mathbf{R}'}$, the Lindblad jump operator becomes $\hat{L}_{\mathbf{R}} = \sqrt{\gamma} \hat{b}_{\mathbf{R}}^2$. It also yields for the momentum-dependent function:

$$\mathcal{A}_{\mathbf{k}}(t) = 4J \sin^2(k/2) + \mathcal{B}_{\mathbf{k}}(t); \quad (11)$$

$$\mathcal{B}_{\mathbf{k}}(t) = \frac{U}{L} \sum_{\mathbf{q}} G_{\mathbf{q}}(t) = U\bar{n}(t); \quad (12)$$

$$\mathcal{F}_{\mathbf{q}} = \frac{4\gamma}{L}; \quad (13)$$

$$\mathcal{G}_{\mathbf{q}} = \frac{\gamma}{L}, \quad (14)$$

$$\mathcal{H}_{\mathbf{q}} = 0. \quad (15)$$

Finally, the set of EoMs at Eq. (5) can be simplified using the previous relations and it yields:

$$\frac{d}{dt}G_0(t) = -\frac{\gamma}{L} \sum_{q \neq 0} (F_0(t)F_q(t)^* + \text{h.c.}) - \frac{4\gamma}{L} G_0(t) \sum_{q \neq 0} G_q(t) - \frac{2\gamma}{L} G_0(t)(G_0(t) - 1); \quad (16a)$$

$$\frac{d}{dt}F_0(t) = -\frac{\gamma}{L} (2G_0(t) - 3)F_0(t) - \frac{4\gamma}{L} F_0(t) \sum_{q \neq 0} G_q(t) - \frac{\gamma}{L} (2G_0(t) + 1) \sum_{q \neq 0} F_q(t); \quad (16b)$$

$$\frac{d}{dt}G_k(t) = -2\mathcal{B}_k(t) \text{Im}(F_k(t)) - \frac{\gamma}{L} (F_0(t)F_k(t)^* + \text{h.c.}) - \frac{4\gamma}{L} G_0(t)G_k(t), \quad \forall k \neq 0; \quad (16c)$$

$$\frac{d}{dt}F_k(t) = -\left[2i\mathcal{A}_k(t) + \frac{4\gamma}{L}G_0(t)\right]F_k(t) - \left[i\mathcal{B}_k(t) + \frac{\gamma}{L}F_0(t)\right](2G_k(t) + 1), \quad \forall k \neq 0, \quad (16d)$$

where the initial conditions for the condensate mode $k = 0$ and the modes $k \neq 0$ are given by:

$$G_0(0) = N_0 = N - \sum_{k \neq 0} G_k(0); \quad (17a)$$

$$F_0(0) = \Theta(U)N_0; \quad (17b)$$

$$G_k(0) = \frac{1}{2} \left(\frac{\mathcal{A}_k}{\mathcal{E}_k} - 1 \right); \quad (17c)$$

$$F_k(0) = -\frac{\mathcal{B}_k}{2\mathcal{E}_k}, \quad (17d)$$

with $\Theta(U)$ denoting the Heaviside function defined as $\Theta(U) = 1$ if $U > 0$ and $\Theta(U) = 0$ if $U = 0$. The low-lying excitation spectrum \mathcal{E}_k and the coefficients \mathcal{A}_k and \mathcal{B}_k are given by:

$$\mathcal{E}_k = \sqrt{\mathcal{A}_k^2 - \mathcal{B}_k^2}, \quad \mathcal{A}_k = 4J \sin^2(k/2) + \mathcal{B}_k, \quad \mathcal{B}_k = U\bar{n}. \quad (18)$$

3 Quench dynamics of the isolated Bose-Hubbard chain

In Ref. [59], the validity of the EoM approach to describe accurately the quench dynamics of the dissipative BH chain characterized by on-site (or long-range) two-body losses and initially confined in the SF phase has been certified against tensor networks numerical simulations. Hence, we can rely on the latter to describe the quench dynamics of the isolated BH chain in this same gapless phase for a sudden global quench on the interaction strength U . However, due to this new framework, the theory requires several adjustments. In what follows, we present them and benchmark the theoretical predictions of the EoM approach with those provided by a quasiparticle theory proposed in Ref. [57, 68].

In what follows, a sudden global quench on the interaction strength U is performed for the isolated BH chain confined in the SF phase. To do so, the set of EoMs has to be slightly modified:

- The quantum system being isolated has $U(1)$ symmetry, i.e. particle-number conservation, implying that the momentum- and time-dependent functions $\mathcal{A}_k(t)$ and $\mathcal{B}_k(t)$ depending on $n(t)$ remain constant in time and become equal to their initial value.
- The coefficients \mathcal{A}_k and \mathcal{B}_k in the EoMs have to be replaced by $\mathcal{A}_{k,f}$ and $\mathcal{B}_{k,f}$ taking into account the post-quench value of U denoted by U_f .
- Similarly for the initial conditions, \mathcal{A}_k and \mathcal{B}_k are replaced by $\mathcal{A}_{k,i}$ and $\mathcal{B}_{k,i}$ depending on the pre-quench value U_i .
- $\gamma = 0$ for each EoM in order to remove dissipation effects.

Finally, we get the following set of EoMs:

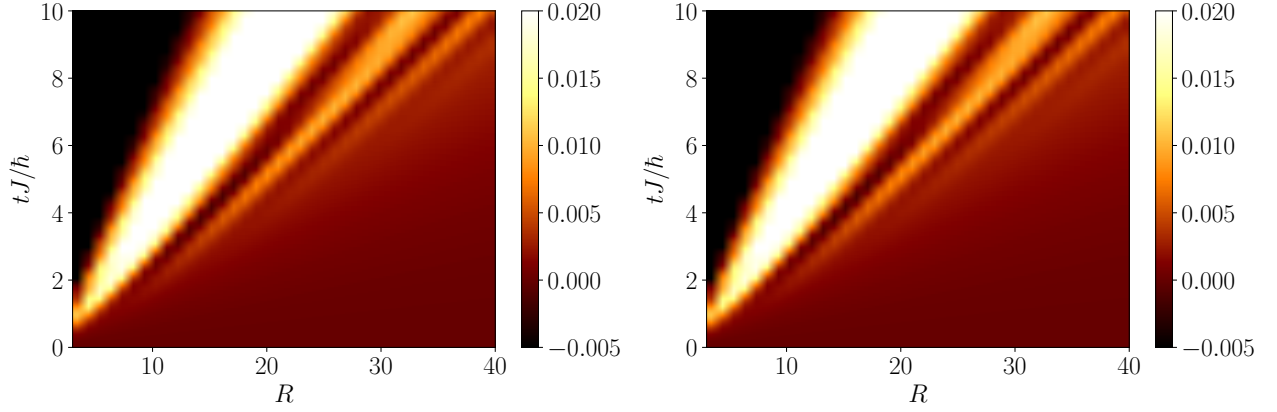


Figure 1: Connected one-body correlation function $G_1(R, t)$ for a sudden global quench on U of the BH chain confined in the SF phase. (top) QP approach (bottom) EoM approach. The considered parameters are: $J = 1$, $U_f = 0.5$, $U_i = 1$, $N = L = 400$.

$$\frac{d}{dt}G_k(t) = -2\mathcal{B}_{k,f}\text{Im}(F_k(t)); \quad (19a)$$

$$\frac{d}{dt}F_k(t) = -2i\mathcal{A}_{k,f}F_k(t) - i\mathcal{B}_{k,f}(1 + 2G_k(t)), \quad (19b)$$

where the initial conditions are defined as follows:

$$G_k(0) = \frac{1}{2} \left(\frac{\mathcal{A}_{k,i}}{\mathcal{E}_{k,i}} - 1 \right); \quad (20)$$

$$F_k(0) = -\frac{\mathcal{B}_{k,i}}{2\mathcal{E}_{k,i}}, \quad (21)$$

with the momentum-dependent pre-quench functions $\mathcal{A}_{k,i}$ and $\mathcal{B}_{k,i}$ and the pre-quench quasiparticle dispersion relation $\mathcal{E}_{k,i}$ having the following form:

$$\mathcal{E}_{k,i} = \sqrt{\mathcal{A}_{k,i}^2 - \mathcal{B}_{k,i}^2}, \quad \mathcal{A}_{k,i} = 4J \sin^2(k/2) + U_i \bar{n}, \quad \mathcal{B}_{k,i} = U_i \bar{n}. \quad (22)$$

Note that if no quench is induced, i.e. $U_i = U_f$, then the EoMs are strictly equal to zero and we recover $F_k(t) = F_k(0)$ and $G_k(t) = G_k(0)$ as expected. In what follows, the connected one-body correlation function $G_1(R, t)$ defined as $G_1(R, t) = \langle \hat{b}_R^\dagger \hat{b}_0 \rangle_t - \langle \hat{b}_R^\dagger \hat{b}_0 \rangle_0$ is considered. In reciprocal space, the latter reads:

$$G_1(R, t) = \frac{1}{L} \sum_{k \neq 0} e^{ikR} (\langle \hat{n}_k \rangle_t - \langle \hat{n}_k \rangle_0) + \frac{1}{L} (\langle \hat{n}_0 \rangle_t - \langle \hat{n}_0 \rangle_0). \quad (23)$$

According to the expression of \hat{H}_f after diagonalisation in reciprocal space, see Refs. [57, 59, 68], the latter can be simplified using the following property:

$$\frac{d\langle \hat{n}_0 \rangle_t}{dt} = i \langle [\hat{H}_f, \hat{n}_0] \rangle_t = 0, \quad (24)$$

meaning that $\langle \hat{n}_0 \rangle_t = \langle \hat{n}_0 \rangle_0$. Then, $G_1(R, t)$ reduces to:

$$G_1(R, t) = \frac{1}{L} \sum_{k \neq 0} \cos(kR) [G_k(t) - G_k(0)], \quad (25)$$

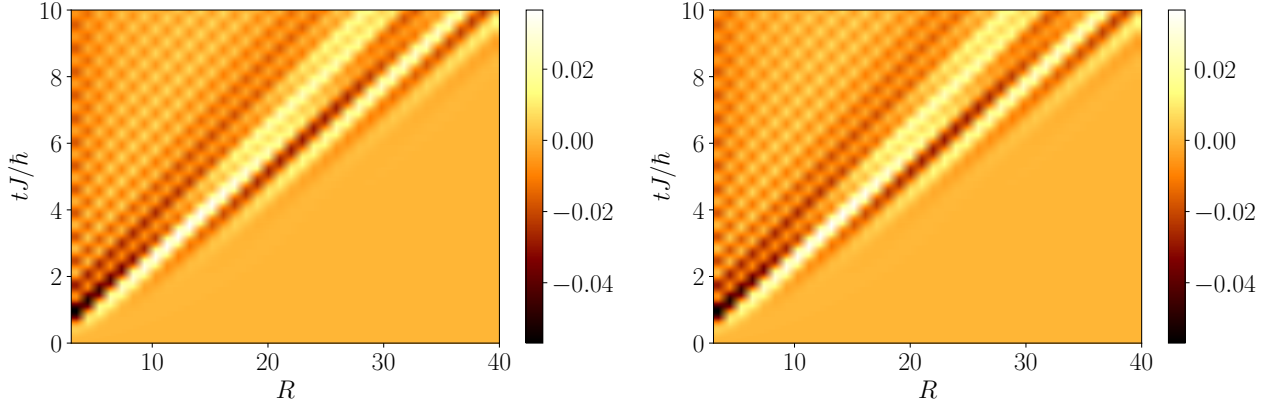


Figure 2: Connected density-density correlation function $G_2(R, t)$ for a sudden global quench on U of the BH chain confined in the SF phase. (top) QP approach (bottom) EoM approach. The considered parameters are: $J = 1$, $U_f = 0.5$, $U_i = 1$, $N = L = 400$.

where $G_k(t)$ was characterised previously. Our EoM approach is compared to a quasiparticle (QP) approach based on the Heisenberg picture together with the introduction of Bogolyubov quasiparticle operators [57, 68]. Its validity has been certified numerically using tensor network based techniques [58]. The QP approach permits to find an explicit expression of $G_1(R, t)$ which reads as:

$$G_1(R, t) = \frac{1}{L} \sum_{k \neq 0} S_k^{(1)} \cos(kR) \sin^2(\mathcal{E}_{k,f} t), \quad S_k^{(1)} = \frac{(\mathcal{A}_{k,i} \mathcal{B}_{k,f} - \mathcal{A}_{k,f} \mathcal{B}_{k,i}) \mathcal{B}_{k,f}}{\mathcal{E}_{k,i} \mathcal{E}_{k,f}^2}, \quad (26)$$

where the amplitude function is denoted by $S_k^{(1)}$. On Fig. 1, both theoretical approaches are compared and we find a perfect agreement between them. This validates the EoM approach defined by the set of coupled differential equations at Eq. (16). Note that both theories are equivalent since they are based on the same expression of the diagonalised form of the Hamiltonian \hat{H} in Fourier space. While the EoM approach is based on the calculation of coupled first-order differential equations of quadratic correlators, the QP approach directly calculates the expression of the time-evolved Bogolyubov quasiparticle operators and thus permits to find an explicit analytical expression of the correlation functions. Regarding the density fluctuations characterised via the G_2 connected density-density correlation function, the latter may be written as follows:

$$G_2(R, t) = \langle \hat{n}_R(t) \hat{n}_0(t) \rangle_c = \langle \hat{n}_R \hat{n}_0 \rangle_t - \langle \hat{n}_R \rangle_t \langle \hat{n}_0 \rangle_t - \langle \hat{n}_R \hat{n}_0 \rangle_0 + \langle \hat{n}_R \rangle_0 \langle \hat{n}_0 \rangle_0. \quad (27)$$

Relying on the mean-field approximation, G_2 reads as:

$$G_2(R, t) = \frac{2\bar{n}}{L} \sum_{k \neq 0} \cos(kR) [\text{Re}(F_k(t)) - \text{Re}(F_k(0)) + G_k(t) - G_k(0)]. \quad (28)$$

Note that $G_1(R, 0) = G_2(R, 0) = 0$ as expected since both G_1 and G_2 refer to the connected version of the one-body and density-density correlation function respectively. The previous analytical expression of $G_2(R, t)$ is consistent with Ref. [59] where the following expression is found:

$$g_2(R, t) = n(t)^2 + \frac{2n(t)}{L} \sum_{k \neq 0} \cos(kR) [\text{Re}(F_k(t)) + G_k(t)], \quad (29)$$

where $g_2(R, t) = \langle \hat{n}_R \hat{n}_0 \rangle_t$ denotes the non-connected density-density correlation function in the SF-mean-field regime while considering loss processes via a time-dependent density $n(t)$. The latter expression also relies on the mean-field approximation. By considering particle-number conservation, i.e. $n(t) = n = \bar{n}$, for the isolated BH chain and according to the definition of G_2 and g_2 , we can deduce that $G_2(R, t) = g_2(R, t) - g_2(R, 0)$. Hence, we find:

$$G_2(R, t) = g_2(R, t) - g_2(R, 0) = \bar{n}^2 + \frac{2\bar{n}}{L} \sum_{k \neq 0} \cos(kR) [\text{Re}(F_k(t)) + G_k(t)] - \bar{n}^2 - \frac{2\bar{n}}{L} \sum_{k \neq 0} \cos(kR) [\text{Re}(F_k(0)) + G_k(0)], \quad (30)$$

leading finally to the expected expression of G_2 at Eq. (28). Note that the connected part of the G_2 correlation function namely $-\langle \hat{n}_R \rangle_t \langle \hat{n}_0 \rangle_t + \langle \hat{n}_R \rangle_0 \langle \hat{n}_0 \rangle_0$ vanishes for the isolated BH chain. Indeed, according to Ref. [59], in the presence of particle losses the G_1 (non-connected) one-body correlation function also called one-body density matrix is defined and takes the following form in the SF-mean-field regime:

$$G_1(R, t) = \langle \hat{b}_R^\dagger \hat{b}_0 \rangle_t = n(t) = G_1(0, t) = \langle \hat{n}_0 \rangle_t, \quad (31)$$

where the mean-field approximation has been considered to deduce the latter form being spatial-independent. Using the translational invariance of the model, we end up with $\langle \hat{n}_0 \rangle_t = \langle \hat{n}_R \rangle_t$, $\forall R \in \mathbb{N}$. Finally, for the isolated BH chain, we have $\langle \hat{n}_0 \rangle_t = \langle \hat{n}_R \rangle_t = \bar{n} = \langle \hat{n}_0 \rangle_0 = \langle \hat{n}_R \rangle_0$ and thus we recover that the connected part of G_2 vanishes as expected.

The G_2 equal-time connected density-density correlation function at Eq. (28) is deduced theoretically by injecting the quadratic bosonic correlators F and G by their values obtained by solving their respective EoM. The second theoretical approach is given by the QP theory, see Ref. [68], leading to:

$$G_2(R, t) = \frac{1}{L} \sum_{k \neq 0} \mathcal{S}_k^{(2)} \cos(kR) \sin^2(\mathcal{E}_{k,f}t), \quad \mathcal{S}_k^{(2)} = \frac{2\bar{n} (\mathcal{A}_{k,f} \mathcal{B}_{k,i} - \mathcal{A}_{k,i} \mathcal{B}_{k,f})}{(\mathcal{A}_{k,f} + \mathcal{B}_{k,f}) \mathcal{E}_{k,i}}. \quad (32)$$

On Fig. 2, both theoretical approaches are compared and we find a perfect agreement between them. This validates for another observable the EoM approach defined by the set of coupled differential equations at Eq. (16). Note that the set of EoMs at Eq. (19) is valid for the Hamiltonian \hat{H} associated to the BH chain. In the SF-mean-field regime, the latter can be expressed in the generic quadratic Bose form when considering the reciprocal space:

$$\hat{H} = \frac{1}{2} \sum_{k \neq 0} \mathcal{A}_k (\hat{b}_k^\dagger \hat{b}_k + \hat{b}_{-k} \hat{b}_{-k}^\dagger) + \mathcal{B}_k (\hat{b}_k^\dagger \hat{b}_{-k}^\dagger + \hat{b}_k \hat{b}_{-k}) = \frac{1}{2} \sum_{k \neq 0} (\hat{b}_k^\dagger \quad \hat{b}_{-k}) \hat{H}_{\text{BdG}}(k) \begin{pmatrix} \hat{b}_k \\ \hat{b}_{-k}^\dagger \end{pmatrix}, \quad \hat{H}_{\text{BdG}}(k) = \begin{pmatrix} \mathcal{A}_k & \mathcal{B}_k \\ \mathcal{B}_k & \mathcal{A}_k \end{pmatrix}, \quad (33)$$

with $\mathcal{A}_k = 4J \sin^2(k/2) + U\bar{n}$ and $\mathcal{B}_k = U\bar{n}$ [58, 69] and \hat{H}_{BdG} corresponding to the bosonic Bogolyubov-de-Gennes Hamiltonian. Similar statements are expected to apply for Hamiltonians which can be cast into the previous form and involving a fermionic Bogolyubov-de-Gennes Hamiltonian.

By considering the thermodynamic limit, i.e. $L \rightarrow +\infty$, and by performing some trivial algebra, for both connected equal-time correlation functions can be expressed in the following generic form [57]:

$$G_1(R, t) \sim \int_{\mathcal{B}} dk \mathcal{S}_k^{(i)} \{ e^{i(kR+2\mathcal{E}_{k,f}t)} + e^{i(kR-2\mathcal{E}_{k,f}t)} \}, \quad (34)$$

where $\mathcal{B} = [-\pi, \pi]$ denotes the first Brillouin zone. Note that the latter form unveiled at Ref. [57] will be essential for the discussion about the quench spectroscopy method (QS) applied to the dissipative Bose-Hubbard chain. More precisely, Eq. (37) consists in the generic form of equal-time connected correlation functions (ETCCF) for an isolated quantum lattice model driven out of equilibrium via a weak sudden global quench. In Ref. [57], the large distance and time behavior of the latter expression is characterized using the stationary phase approximation to unravel general statements regarding the correlation spreading in closed quantum systems. For short-range interacting quantum models, the space-time pattern of ETCCFs is expected to display a twofold linear structure. This double structure is characterised by a ballistic, i.e. linear, correlation edge (CE) separating the causal region of the correlations from the non-causal one. The causal region refers to the region where the correlations are different from zero. In other words, beyond the CE, the space-time correlations are exponentially suppressed. The second structure consists in the ballistic spreading of a series of local maxima and minima in the vicinity of the CE. The CE velocity is given by twice the maximal group velocity corresponding to the quasiparticle pair with the highest velocity, i.e. $V_{\text{CE}} = 2V_g(k^*) = 2\max(d\mathcal{E}_{k,f}/dk)$ with $k^* = \text{argmax}(d\mathcal{E}_{k,f}/dk)$. The velocity associated to the linear spreading of the

local extremum is given by twice the phase velocity evaluated at the quasimomentum for which the group velocity is maximal, i.e. $V_m = 2V_\varphi(k^*) = 2\mathcal{E}_{k^*}/k^*$. The validity of the latter behaviour has been certified both analytically [57,68] and numerically using whether time-dependent matrix product state calculations [58] or time-dependent variational Monte-Carlo calculations [55].

4 Double quench dynamics of the Bose-Hubbard chain

In what follows, we investigate the behaviour of $G_2(R, t)$ for a sudden global quench not only on the dissipation strength from $\gamma = 0$ to $\gamma > 0$ but also on the interaction strength U from $U = U_i$ to $U = U_f$ such that the BH chain is initially confined in the SF phase. Experimentally, the quench on U can be realised in ultracold-atom experiments by suddenly lowering or raising the depth of the optical lattice in order to decrease or to increase the dimensionless interaction parameter U/J respectively [3]. In this context, the EoMs at Eq. (16) as well as the corresponding initial conditions at Eq. (17d) have to be slightly modified. In the EoMs, \mathcal{A}_k and \mathcal{B}_k are replaced by $\mathcal{A}_{k,f}$ and $\mathcal{B}_{k,f}$ depending now on the post-quench interaction strength U_f . For the initial conditions, \mathcal{A}_k and \mathcal{B}_k are replaced by $\mathcal{A}_{k,i}$ and $\mathcal{B}_{k,i}$ depending now on the pre-quench interaction strength U_i . G_2 the ETCCF to investigate density fluctuations is computed by solving the previous set of EoMs whose values of the relevant correlators are injected in the theoretical expression of g_2 given by:

$$g_2(R, t) = n(t)^2 + \frac{2n(t)}{L} \sum_{k \neq 0} \cos(kR) [G_k(t) + \text{Re}(F_k(t))]. \quad (35)$$

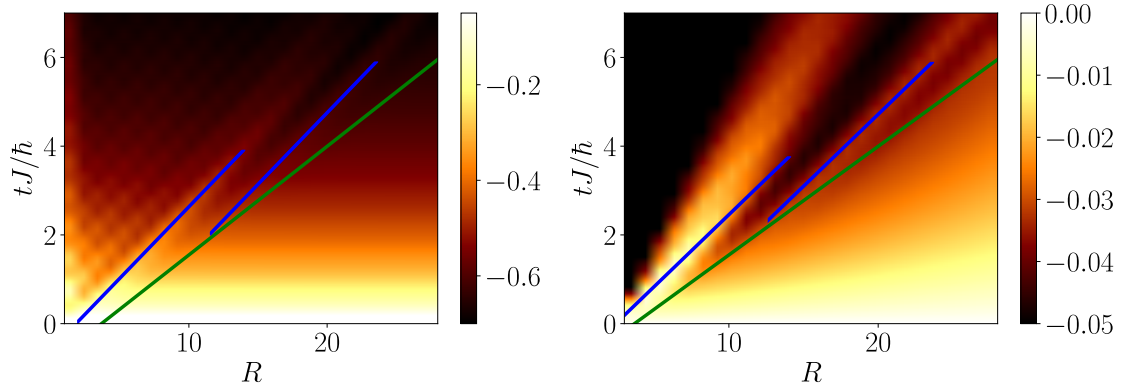


Figure 3: Space-time pattern of (left) $G_2(R, t) = \langle \hat{n}_R(t) \hat{n}_0(t) \rangle_c$ (right) $G_1(R, t) = \langle \hat{b}_R^\dagger \hat{b}_0 \rangle_t - \langle \hat{b}_R^\dagger \hat{b}_0 \rangle_0$ for a sudden global quench on the dissipation strength from $\gamma = 0$ to $\gamma > 0$ and on the two-body repulsive interaction strength U from $U = U_i$ to $U = U_f$ such that the quantum system is initially confined in the SF phase. The solid green line represents the correlation edge (CE) propagating linearly at the velocity $V_{CE} = 2V_g(k^*) = 2\max(d\mathcal{E}_{k,f}/dk)$. The solid blue line represents the ballistic spreading of the series of local maxima and minima in the vicinity of the CE at the velocity $V_m = 2V_\varphi(k^*) = 2\mathcal{E}_{k^*,f}/k^*$. The parameters are: $N(0) = L = 400$ to satisfy the thermodynamic limit, $J = 1$, $U_f = 0.5$, $U_i = 2$, $\gamma = 0.1$. For the twofold linear structure induced by the quench on the interactions to be visible, the amplitudes of both patterns have been saturated.

The latter is plotted on Fig. 3 and we clearly see the effect of each quench individually. The quench on U gives rise to a twofold linear structure characterised by a correlation edge (CE) propagating ballistically at twice the maximal group velocity. The second structure consists in a series of local maxima and minima spreading also ballistically in the vicinity of the CE at twice the phase velocity evaluated at the quasimomentum for which the group velocity is maximal. This is reminiscent of the behaviour of G_2 for a sudden global quench on the interaction strength U for the isolated BH chain confined in the SF phase. We can thus deduce from the previous findings that the algebraic decay in time of G_2 , thus independent on the lattice site index R , corresponds to the signature of the quench on the dissipation strength γ . The latter effect is clearly visible in the background of Fig. 3. Similar statements are also valid for the G_1 ETCCF on Fig. 3 where G_1 has the following expression since $\langle \hat{n}_0 \rangle_t$ is not a conserved quantity anymore (see Eq. (23)):

$$G_1(R, t) = \frac{1}{L} [\langle \hat{n}_0 \rangle_t - \langle \hat{n}_0 \rangle_0 + \sum_{k \neq 0} \cos(kR) (\langle \hat{n}_k \rangle_t - \langle \hat{n}_k \rangle_0)] = \frac{1}{L} \{G_0(t) - G_0(0) + \sum_{k \neq 0} \cos(kR) [G_k(t) - G_k(0)]\}. \quad (36)$$

5 Quench spectroscopy of the double-quenched Bose-Hubbard chain

In Refs. [7, 8, 68], the so-called quench spectroscopy (QS) method has been introduced theoretically whose predictions have been verified numerically using tensor-network-based techniques for one-dimensional quantum systems. The latter permits to determine the low-lying excitation spectrum or quasiparticle dispersion relation of quantum lattice models by analysing their dynamical response to a sudden quench which can be either local, i.e. the perturbation is applied on a specific lattice site, or global, i.e. all the lattice sites are concerned. For instance, it has been applied to disordered quantum lattice models [70, 71]. In what follows, we focus on the case of sudden global quenches. The main feature of this method corresponding also to the most restrictive condition is to consider a so-called weak quench meaning that the many-body ground state of the post-quench Hamiltonian has to be relatively closed to, i.e. strongly overlaps with, the initial state corresponding the ground state of the pre-quench Hamiltonian. In other words, the method holds for sudden global quenches confined in a same gapless or gapped phase and ideally in the same regime within this quantum phase. According to the QP theory used previously and detailed in Refs. [57, 68], equal-time connected correlation functions can generally be cast into a generic form. The latter reads as:

$$G(R, t) = \int_{\mathcal{B}} dk \mathcal{S}_k \{e^{i(kR+2\mathcal{E}_k t)} + e^{i(kR-2\mathcal{E}_k t)}\}, \quad (37)$$

where \mathcal{E}_k refers to the quasiparticle dispersion relation of the post-quench Hamiltonian. The so-called quench spectral function (QSF) denoted by $S_k(\omega)$ is defined as the 1 + 1 (space-time) Fourier transform of the equal-time connected correlation function $G(R, t)$ and reads as [8]:

$$S_k(\omega) = \int_0^L dR \int_0^T dt G(R, t) e^{-i(kR+\omega t)}, \quad (38)$$

where T corresponds to the observation time and L the system size or equivalently the total number of lattice sites. Inserting the generic form of $G(R, t)$ at Eq. (37) in the definition of the QSF at Eq. (38), it yields in the thermodynamic limit, i.e. $L \rightarrow +\infty$, and in the limit of a large observation time, i.e. $T \rightarrow +\infty$, the following theoretical expression:

$$S_k(\omega) = \mathcal{S}_k [\delta(\omega + 2\mathcal{E}_k) + \delta(\omega - 2\mathcal{E}_k)]. \quad (39)$$

As expected, the previous form of the QSF clearly permits to determine the post-quench low-lying excitation spectrum \mathcal{E}_k . Indeed, from Eq. (39), $S_k(\omega)$ represents twice the post-quench quasiparticle dispersion relation $2\mathcal{E}_k$. More precisely, the latter will display the two branches $2E_k$ and $-2E_k$. The prefactor 2 comes from the weak sudden global quench dynamics of the quantum lattice model being mediated by the spreading of quasiparticle pairs. The weight associated to each momentum-dependent energy is characterised by the amplitude function \mathcal{S}_k depending on the quench parameters as well as the observable defining the equal-time correlation function $G(R, t)$. According to Eq. (39), the QSF has $k/-k$ symmetry; the latter coming from the post-quench quasiparticle dispersion relation \mathcal{E}_k and is $\omega/-\omega$ symmetric due to the parity of the Dirac delta function δ .

For the case study of the BH chain submitted to a double quench, the ETCCF G_2 can be reformulated as follows:

$$G_2(R, t) = G_2^U(R, t) + G_2^\gamma(R, t) = G_2^U(R, t) + G_2^\gamma(0, t), \quad (40)$$

where $G_2^U(R, t)$ and $G_2^\gamma(R, t)$ refers to the individual contribution for G_2 due to the weak sudden global quench on the repulsive interaction strength U and the dissipation rate γ respectively. The first equality is valid according to the previous findings (see Fig. 3 and the associated discussion) where both quantum quenches seem to be independent. The second one comes from the fact that the quench on γ leads to a spatial-independent correlation spreading as depicted on Fig. 3. Indeed, from Ref. [59] where an unique quench on the dissipation strength γ is considered, $G_2^\gamma(R, t)$ reads as (see also Eq. (35)):

$$G_2^\gamma(R, t) = g_2^\gamma(R, t) - g_2^\gamma(R, 0); \quad (41)$$

$$G_2^\gamma(R, t) = n(t)^2 + \frac{2n(t)}{L} \sum_{k \neq 0} \cos(kR) [G_k(t) + \text{Re}(F_k(t))] - n(0)^2 - \frac{2n(0)}{L} \sum_{k \neq 0} \cos(kR) [G_k(0) + \text{Re}(F_k(0))]. \quad (42)$$

For the BH chain in the SF-mean-field, the first excitations having a momentum $k = 0^+$ are the relevant ones. This implies that the associated wavelength λ is much higher than the lattice spacing a , i.e. $\lambda \gg a$. Hence, it follows that the discretization of the lattice is irrelevant and thus that the contribution $G_2^\gamma(R, t)$ is spatially independent, i.e. $G_2^\gamma(R, t) = G_2^\gamma(0, t)$. This can be verified straightforwardly by injecting $k = 0^+$ in Eq. (40). Finally, it immediately follows from Eq. (40) that:

$$S_k(\omega) = S_k^U(\omega) + S_{k=0}^\gamma(\omega). \quad (43)$$

Therefore, the consequence of the quench on γ for the quench spectral function is minimal according to Eq. (43). Indeed, the latter will increase the amplitude of $S_k(\omega)$ for the quasimomentum $k = 0$ for any energy ω . This effect is shown on Fig. 4. On Fig. 4, the QSFs associated to the G_2 and G_1 ETCCF are displayed and are benchmarked with twice the post-quench quasiparticle dispersion relation associated to the isolated BH chain confined in the SF-mean-field regime, i.e. $2\mathcal{E}_k$, having the following expression (see also Eq. (18)):

$$2\mathcal{E}_{k,f} = 4\sqrt{2J \sin^2(k/2) (2J \sin^2(k/2) + U_f \bar{n})}, \quad (44)$$

where $\bar{n} = N(0)/L$ refers here to the initial filling of the lattice chain where $N(0)$ denotes the initial total number of bosonic particles on the lattice. Note that for G_1 , the spatial dependence of the contribution due to the quench on the dissipations, i.e. $G_1^\gamma(R, t)$, becomes slightly relevant as suggested on Fig. 3. This results in non-zero amplitudes for the associated QSF for a momentum k in the limit $k \rightarrow 0$ and for any energy ω . The latter is consistent with the fact that the first excitations have a momentum close to zero.

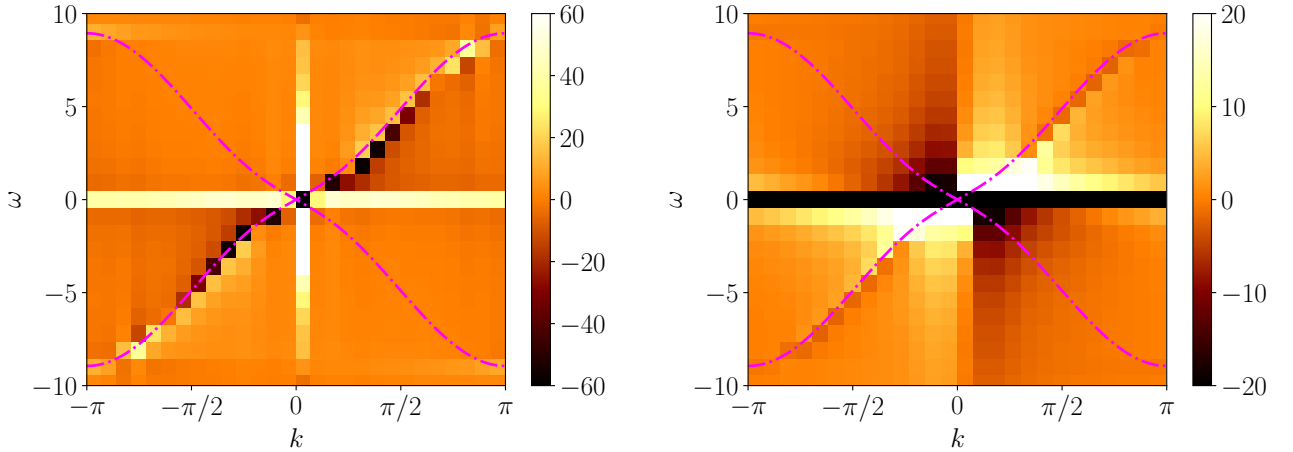


Figure 4: Quench spectral function $S_k(\omega)$ associated to (left) $G_2(R, t) = \langle \hat{n}_R(t) \hat{n}_0(t) \rangle_c$ the equal-time connected density-density correlation function (right) $G_1(R, t) = \langle \hat{b}_R^\dagger \hat{b}_0 \rangle_t - \langle \hat{b}_R^\dagger \hat{b}_0 \rangle_0$ the equal-time connected one-body correlation function. A double quench comprising not only a weak sudden global quench on the dissipation strength from $\gamma = 0$ to $\gamma > 0$ but also another one on the two-body repulsive interaction strength U from $U = U_i$ to $U = U_f$ is considered such that the quantum system is confined in the SF phase. The dashed-dotted magenta lines represent twice and minus twice the post-quench quasiparticle dispersion relation associated to the isolated BH chain confined in the SF-mean-field regime, i.e. $2\mathcal{E}_{k,f}$ and $-2\mathcal{E}_{k,f}$ respectively, see Eq. (44). Note that half of the two low-lying excitation spectra are missing resulting in a loss of the $k/-k$ and $\omega/-\omega$ symmetries. Indeed, the latter would be characterized by a negative group velocity and only the correlation pattern with $R, t \geq 0$ is considered here. To recover the second half, the space-time region of the correlation pattern with $R \leq 0$ and $t \geq 0$ has to be considered. The considered parameters to plot both QSFs are: $\bar{n} = 1$ with $N(0) = L = 400$ to satisfy the thermodynamic limit, $J = 1$, $U_i = 2$, $U_f = 0.5$, $\gamma = 0.1$.

We move on to the case of strong dissipations implying large γ . The aim of this investigation is to certify the validity of the QS approach for strong loss processes. On Fig. 5, we consider a dissipation strength ten times higher than

previously for the double-quenched BH chain confined in the SF phase. We notice that the QSF is well benchmarked by the twice (or minus twice) $\mathcal{E}_{k,f}$ the theoretical quasiparticle dispersion relation associated to the post-quench Hamiltonian of the BH chain confined in the SF phase. Consequently, this permits to state that the QS method can still be applied in the framework of strong loss processes.

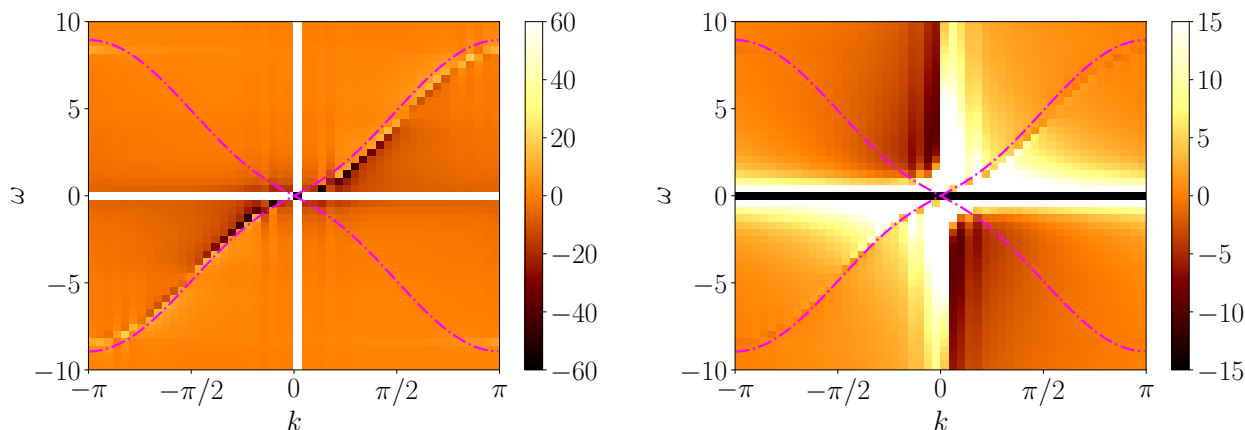


Figure 5: Quench spectral function $S_k(\omega)$ associated to (left) $G_2(R, t) = \langle \hat{n}_R(t) \hat{n}_0(t) \rangle_c$ the equal-time connected density-density correlation function (right) $G_1(R, t) = \langle \hat{b}_R^\dagger \hat{b}_0 \rangle_t - \langle \hat{b}_R^\dagger \hat{b}_0 \rangle_0$ the equal-time connected one-body correlation function. A weak sudden double quench is performed on the dissipation strength from $\gamma = 0$ to $\gamma > 0$ as well as on the two-body repulsive interaction strength U from $U = U_i$ to $U = U_f$ such that the quantum system is confined in the SF phase. The dashed-dotted magenta lines represent twice and minus twice the post-quench quasiparticle dispersion relation associated to the isolated BH chain confined in the SF-mean-field regime, i.e. $2\mathcal{E}_{k,f}$ and $-2\mathcal{E}_{k,f}$ respectively, see Eq. (44). The parameters are: $\bar{n} = 1$ with $N(0) = L = 400$ to satisfy the thermodynamic limit, $J = 1$, $U_i = 2$, $U_f = 0.5$, $\gamma = 1$.

We turn to the case of large post-quench interaction strength denoted by U_f while considering small dissipations, i.e. $\gamma \ll 1$. For large enough U_f , the 1D BH model is no longer confined in the mean-field regime of the SF phase but in the strongly-correlated regime. Indeed, the mean-field condition given by $\bar{n} \gg U/J$ is no longer satisfied when the dimensionless parameter U/J and the filling of the lattice \bar{n} have approximately the same value. In what follows, we consider the specific case where $J = U_f = \bar{n} = N(0)/L$. However, from Ref. [58], it has been shown that the quasiparticle dispersion relation \mathcal{E}_k for the BH chain confined in the SF-mean-field regime defined at Eq. (44) remains accurate far beyond its validity domain. Hence, even at large post-quench interaction strength U_f , we should be able to rely on the QS approach in order to get an accurate description of the low-lying excitation spectrum of the 1D BH model confined in the SF-strongly-correlated regime. On Fig. 6, the QSF associated to the density fluctuations via the ETCCF G_2 and to the phase fluctuations via G_1 are compared to the theoretical expression of $\mathcal{E}_{k,f}$ initially valid in the SF-mean-field. A very good benchmark is found for both QSFs.

We stress that all the previous findings do not apply for sudden global quenches confined in the MI phase. Indeed, to generate the corresponding low-lying excitations, it requires to consider a subspace of the full Hilbert space where the $U(1)$ particle-number symmetry is conserved during the dynamics. Hence, in the presence of loss processes, the latter is broken and the quantum system remains in the SF phase independently of the strength of the repulsive interactions due to the incommensurate filling of the lattice chain.

6 Experimental feasibility of the quench spectroscopy method

The QS presents several difficulties of applicability and limits from an experimental point of view. Indeed, in the context of the dissipative BH chain, the main limitations are the following:

- The restrictive choice for the observables in order to compute the associated connected equal-time correlation function.
- The different sources of noise including the shot and technical noise.

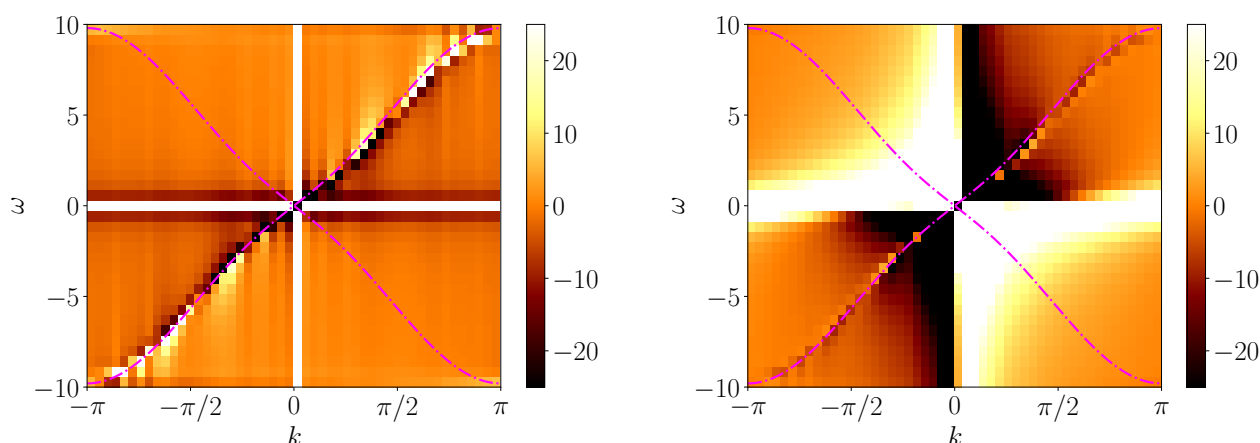


Figure 6: Quench spectral function $S_k(\omega)$ associated to (left) $G_2(R, t) = \langle \hat{n}_R(t) \hat{n}_0(t) \rangle_c$ the equal-time connected density-density correlation function (right) $G_1(R, t) = \langle \hat{b}_R^\dagger \hat{b}_0 \rangle_t - \langle \hat{b}_R^\dagger \hat{b}_0 \rangle_0$ the equal-time connected one-body correlation function. A weak sudden double quench is performed on the dissipation strength from $\gamma = 0$ to $\gamma > 0$ as well as on the two-body repulsive interaction strength U from $U = U_i$ to $U = U_f$ such that the quantum system is confined in the strongly-correlated regime of the SF phase. The dashed-dotted magenta lines represent twice and minus twice the post-quench quasiparticle dispersion relation associated to the isolated BH chain confined in the SF-mean-field regime, i.e. $2\mathcal{E}_{k,f}$ and $-2\mathcal{E}_{k,f}$ respectively, see Eq. (44). The parameters are: $\bar{n} = 1$ with $N(0) = L = 400$ to satisfy the thermodynamic limit, $J = 1$, $U_i = 2$, $U_f = 1$, $\gamma = 0.1$.

- The difficulty for the imaging due to the coherence of the time-evolved quantum state when considering the gapless SF phase contrary to the gapped MI phase.
- The resolution associated to the experimental data to describe accurately the causal region of the space-time correlations. The latter region is primordial to recover the full information regarding the low-lying excitation spectrum of the quantum lattice model. Indeed, reliable experimental data on the correlation edge, which is already not an easy task for experimentalists, is not sufficient. The latter contains only information on the quasiparticle pair propagating with the fastest group velocity.
- From a more general viewpoint, a main limit of the QS method is to be valid and reliable for weak global quenches. This "quench weakness" implies difficulties for experimentalists. To illustrate the previous difficulty, a strong global quench confined in the MI phase is much easier to handle compared to a weak quench in the same phase. Indeed, for the imaging and more precisely for the mobility of the bosonic particles, a strong global quench is necessary. By "strong quench", we mean here that the initial or pre-quench dimensionless interaction parameter is significantly higher or lower than the final or post-quench dimensionless interaction parameter, i.e. $(U/J)_i \gg (\ll) (U/J)_f$.
- Another limitation of the method lies in the kind of loss processes which is considered. It is entirely possible to imagine loss processes leading to a non-trivial, i.e. strong, spatial dependence for the space-time pattern of the ETCCF

The latter QS method to probe low-lying excitation spectra can be extended to dissipative many-body quantum fermionic and spin lattice chains, to a higher dimensionality of the lattice and to long-range interactions. Most importantly, this technique can be applied to experimental measurements obtained using quantum simulators based on ultracold atoms to engineer bosonic lattice models, neutral Rydberg atoms or trapped ions for the simulation of fermionic and spin lattice models. To conclude, QS can be seen as an alternative approach to the standard experimental techniques to measure excitation spectra such as the angle-resolved photoemission spectroscopy (ARPES) [72] or Bragg spectroscopy [73].

7 Applicability of the quench spectroscopy to a non-Hermitian quantum lattice model

We focus here on the case study of the $s = 1/2$ non-Hermitian transverse-field Ising model (TFIM) on a one-dimensional chain of L lattice sites whose lattice spacing is still fixed to unity, i.e. $a = 1$; for simplicity, we still consider $\hbar = 1$. The corresponding Hamiltonian \hat{H} reads:

$$\hat{H} = J \sum_R \hat{S}_R^x \hat{S}_{R+1}^x - (h + i\gamma) \sum_R \hat{S}_R^z, \quad (45)$$

where \hat{S}_R^α corresponds to the $s = 1/2$ spin operator acting on the lattice site R along the $\alpha \in \{x, z\}$ axis. $J > 0$ refers to the antiferromagnetic spin exchange coupling between nearest neighbors spins, $h > 0$ is the constant and homogeneous transverse magnetic field and γ denotes the dissipative strength representing the local dephasing noise. In what follows, we consider $\gamma > 0$ as well as the paramagnetic phase (also called z polarized phase in the literature) where the spins are polarized along z axis, i.e. are aligned with the magnetic field, for $h \gg J$. In Ref. [74], *J.Despres et al.* studied the quasiparticle dispersion relation as well as the quench dynamics of this non-Hermitian spin model in the paramagnetic phase. Regarding the low-lying excitation spectrum, they relied on the following Holstein-Primakoff (HP) transformation:

$$\hat{S}_R^x = \frac{\hat{a}_R + \hat{a}_R^\dagger}{2}; \quad (46a)$$

$$\hat{S}_R^y = \frac{\hat{a}_R - \hat{a}_R^\dagger}{2i}; \quad (46b)$$

$$\hat{S}_R^z = \frac{1}{2} - \hat{a}_R^\dagger \hat{a}_R, \quad (46c)$$

where \hat{a}_R (\hat{a}_R^\dagger) refers to the annihilation (creation) bosonic operator acting on the lattice site R . The latter obey canonical commutation relations. This HP transformation implies to consider a regime in which the bosonic local occupation number remains small, i.e. $\langle \hat{a}_R^\dagger \hat{a}_R \rangle \ll 1$, which is the case for example in the paramagnetic phase of the TFIM at equilibrium. This transformation permits to express \hat{H} at Eq. (45) in the generic quadratic Bose form discussed at Eq. (33) with $\mathcal{A}_k = h + i\gamma + \mathcal{B}_k$ and $\mathcal{B}_k = (J/2) \cos(k)$. Note that here the value $k = 0$ is included in the summation over the momentum.

To investigate the quench dynamics of the non-Hermitian TFIM, *J.Despres et al.* derived the EoM associated to the quadratic bosonic correlator $G_k(t) = \langle \hat{a}_k^\dagger \hat{a}_k \rangle_t$ and $F_k(t) = \langle \hat{a}_k \hat{a}_{-k} \rangle_t$ where $\langle \dots \rangle_t = \langle \Psi(t) | \dots | \Psi(t) \rangle$. The time-evolved many-body quantum state $|\Psi(t)\rangle$ reads:

$$|\Psi(t)\rangle = \frac{e^{-i\hat{H}t} |\Psi_0\rangle}{\|e^{-i\hat{H}t} |\Psi_0\rangle\|}, \quad |\Psi_0\rangle = |\Psi(0)\rangle = |\text{GS}(\hat{H}(\gamma = 0))\rangle, \quad (47)$$

where $|\Psi_0\rangle$ denotes the initial many-body quantum state corresponding to the ground state of the Hermitian version of the Hamiltonian \hat{H} , i.e. $\gamma = 0$. Using the latter expression, the EoM associated to the time-dependent expectation value of any observable \hat{A} denoted by $G_A(t) = \langle \Psi(t) | \hat{A} | \Psi(t) \rangle = \langle \hat{A} \rangle_t$ reads as:

$$\frac{d}{dt} G_A(t) = i \langle \hat{H}^\dagger \hat{A} - \hat{A} \hat{H} \rangle_t + i \langle \hat{H} - \hat{H}^\dagger \rangle_t G_A(t). \quad (48)$$

Then, by replacing \hat{A} by $\hat{a}_k^\dagger \hat{a}_k$ for the correlator $G_k(t)$ and by $\hat{a}_k \hat{a}_{-k}$ for $F_k(t)$, the following set of non-linear coupled differential equations has been found:

$$\frac{d}{dt} F_k(t) = 4 \text{Im}(\mathcal{A}_k) F_k(t) G_k(t) - 2i \mathcal{A}_k F_k(t) - i \mathcal{B}_k [1 + 2G_k(t)]; \quad (49a)$$

$$\frac{d}{dt} G_k(t) = -2\mathcal{B}_k \text{Im}(F_k(t)) + 2 \text{Im}(\mathcal{A}_k) (|F_k(t)|^2 + G_k(t) + G_k(t)^2), \quad (49b)$$

whose initial values are given by:

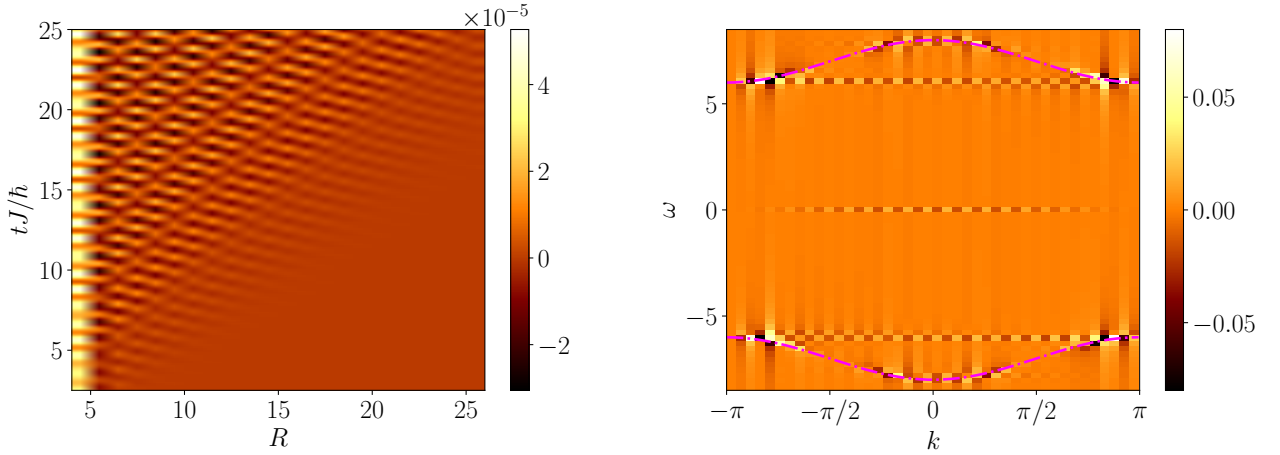


Figure 7: (Left) $G_1(R, t) = \langle \hat{a}_R^\dagger \hat{a}_0 \rangle_t$ the equal-time one-body correlation function (right) the associated quench spectral function $S_k(\omega)$ for a weak sudden global quench on γ from $\gamma = 0$ to $\gamma > 0$ for the non-Hermitian 1D TFIM confined in the paramagnetic (z polarized) phase. The dashed-dotted magenta lines represent twice and minus twice the real part of the momentum-dependent function \mathcal{A}_k , i.e. $2 \operatorname{Re}(\mathcal{A}_k)$ and $-2 \operatorname{Re}(\mathcal{A}_k)$ respectively. For clarity, the space-time correlation pattern of G_1 for the calculation of $S_k(\omega)$ is plotted for $R \geq 0$ and $R \leq 0$ and $t \geq 0$ to recover the second half of the effective quasiparticle dispersion relation. The parameters are: $L = 400$ to reach the thermodynamic limit, $J = 1$, $h = 3.5$ and $\gamma = 0.02$.

$$F_k(0) = \cosh(\alpha_k) \sinh(\alpha_k); \quad (50)$$

$$G_k(0) = \sinh^2(\alpha_k), \quad (51)$$

$$\alpha_k = \frac{1}{2} \operatorname{arctanh} \left(-\frac{\mathcal{B}_k}{\mathcal{A}_k(\gamma=0)} \right). \quad (52)$$

Using the set of EoMs defined at Eq. (49), the correlation spreading induced by the quench on γ is investigated in Ref. [74] by analyzing the equal-time one-body correlation function $G_1(R, t)$ which reads as:

$$G_1(R, t) = \langle \hat{a}_R^\dagger \hat{a}_0 \rangle_t = \frac{1}{L} \sum_k \cos(kR) G_k(t), \quad (53)$$

whose space-time pattern deduced from the previous set of EoMs is qualitatively very well reproduced by the following theoretical guess:

$$G_1(R, t) = \frac{1}{L} \sum_k \mathcal{F}_k^{(1)} \cos(kR) \cos(2 \operatorname{Re}(\mathcal{A}_k)t) \exp(2 \operatorname{Im}(\mathcal{A}_k)t), \quad (54)$$

where $\operatorname{Re}(\mathcal{A}_k) = h + (J/2) \cos(k)$ and $\operatorname{Im}(\mathcal{A}_k) = \gamma$. It immediately follows that $G_1(R, t)$ can be cast into the generic form previously studied. Indeed, after performing some algebra and by considering the thermodynamic limit, i.e. $L \rightarrow +\infty$, we get:

$$G_1(R, t) \sim \int_B dk S_k^{(1)} \{ e^{i(kR+2 \operatorname{Re}(\mathcal{A}_k)t)} + e^{i(kR-2 \operatorname{Re}(\mathcal{A}_k)t)} \}. \quad (55)$$

From Eq. (55) and by performing the Fourier transform, we can easily deduce that only (twice) the real part of the complex low-lying excitation spectrum of the non-Hermitian 1D TFIM will be unveiled by the QSF. Indeed, in the paramagnetic phase, the first band of the spectrum is given by [74]: $\mathcal{E}_k = \operatorname{sgn}(\operatorname{Re}(\mathcal{A}_k)) \sqrt{\mathcal{A}_k^2 - \mathcal{B}_k^2}$. Deep in the latter phase where $h \gg J$, we get: $\mathcal{E}_k = \mathcal{A}_k$ hence $\operatorname{Re}(\mathcal{E}_k) = \operatorname{Re}(\mathcal{A}_k)$. This statement is depicted on Fig. 7 where the QSF probes twice the real part of the quasiparticle dispersion relation $2 \operatorname{Re}(\mathcal{E}_k) = 2 \operatorname{Re}(\mathcal{A}_k)$. The latter investigation permits to certify the applicability and reliability of the QS method for non-Hermitian quantum lattice models and can be straightforwardly extended to non-Hermitian quantum systems subjected to long-range interactions and for a higher dimensionality of the lattice.

8 Conclusion

In this work we have discussed the quench spectroscopy of the open Bose-Hubbard chain confined in the superfluid phase where the dissipation is characterised by on-site two-body losses and of the non-Hermitian transverse-field Ising chain confined in the paramagnetic phase; both from a theoretical point of view.

Regarding the dissipative Bose-Hubbard chain, we have first introduced the theory based on an EoM approach. Then, we benchmarked the latter with a quasiparticle theory for two distinct connected equal-time correlation functions while considering the isolated Bose-Hubbard chain. The latter functions are the G_1 one-body correlation function as well as the G_2 density-density correlation function giving insight regarding the phase and density fluctuations of the quantum model respectively. Then, we investigated the double quench dynamics of the Bose-Hubbard chain where both the repulsive interactions and the dissipations are quenched. Finally, we studied its quench spectroscopy by calculating the quench spectral function associated to G_1 and G_2 . Concerning the non-Hermitian transverse-field Ising chain, we considered the z polarized phase and its associated quench dynamics by considering a equal-time spin-spin correlation function in the aim to apply the quench spectroscopy method to the latter.

This paper unraveled new theoretical results regarding the double quench dynamics of the Bose-Hubbard chain as well as the quench spectroscopy of the dissipative Bose-Hubbard chain which can be confirmed experimentally using quantum simulators based on ultracold atoms. The applicability of the quench spectroscopy method is also extended to non-Hermitian quantum lattice models. To summarize, in the framework of weak sudden global quantum quenches, this paper paves the way to the possibility of applying the quench spectroscopy method to dissipative and non-Hermitian quantum lattice models.

As an extension of the presented research work, the generalizability of the quench spectroscopy approach is an interesting research topic. The latter is likely to be generalized to dissipative fermionic lattice models, dissipative spin lattice models as well as to their reformulation in the continuum and for a higher dimensionality of the lattice or the space respectively. The quench spectroscopy method is also expected to be reliable for dissipative quantum systems involving long-range interactions and for other Lindblad jump operators, i.e. other kind of loss processes.

Acknowledgements

The Author wishes to acknowledge M. Cheneau for fruitful discussions concerning the experimental feasibility of the quench spectroscopy method using cold-atom-based quantum simulators. The Author is also grateful to L. Sanchez-Palencia for useful comments regarding the manuscript.

Funding information This research was supported by Region Ile-de-France in the framework of DIM QuanTip and by the ANR project LOQUST ANR-23-CE47-0006-02.

References

- [1] P. Jurcevic, B. P. Lanyon, P. Hauke, C. Hempel, P. Zoller, R. Blatt and C. F. Roos, *Quasiparticle engineering and entanglement propagation in a quantum many-body system*, Nature **511**, 202 (2014), doi:[10.1038/nature13461](https://doi.org/10.1038/nature13461).
- [2] P. Richerme, Z.-X. Gong, A. Lee, C. Senko, J. Smith, M. Foss-Feig, S. Michalakis, A. V. Gorshkov and C. Monroe, *Non-local propagation of correlations in quantum systems with long-range interactions*, Nature **511**, 198 (2014), doi:[10.1038/nature13450](https://doi.org/10.1038/nature13450).
- [3] M. Cheneau, P. Barmettler, D. Poletti, M. Endres, P. Schauss, T. Fukuhara, C. Gross, I. Bloch, C. Kollath and S. Kuhr, *Light-cone-like spreading of correlations in a quantum many-body system*, Nature (London) **481**, 484 (2012), doi:[10.1038/nature10748](https://doi.org/10.1038/nature10748).
- [4] A. Polkovnikov, K. Sengupta, A. Silva and M. Vengalattore, *Colloquium: Nonequilibrium dynamics of closed interacting quantum systems*, Rev. Mod. Phys. **83**, 863 (2011), doi:[10.1103/RevModPhys.83.863](https://doi.org/10.1103/RevModPhys.83.863).
- [5] C. Gogolin and J. Eisert, *Equilibration, thermalisation, and the emergence of statistical mechanics in closed quantum systems*, Reports on Progress in Physics **79**(5), 056001 (2016), doi:[10.1088/0034-4885/79/5/056001](https://doi.org/10.1088/0034-4885/79/5/056001).
- [6] P. Calabrese and J. Cardy, *Evolution of entanglement entropy in one-dimensional systems*, Journal of Statistical Mechanics: Theory and Experiment **2005**, P04010 (2005), doi:[10.1088/1742-5468/2005/04/P04010](https://doi.org/10.1088/1742-5468/2005/04/P04010).

- [7] L. Villa, J. Despres and L. Sanchez-Palencia, *Unraveling the excitation spectrum of many-body systems from quantum quenches*, Phys. Rev. A **100**, 063632 (2019), doi:[10.1103/PhysRevA.100.063632](https://doi.org/10.1103/PhysRevA.100.063632).
- [8] L. Villa, J. Despres, S. J. Thomson and L. Sanchez-Palencia, *Local quench spectroscopy of many-body quantum systems*, Phys. Rev. A **102**, 033337 (2020), doi:[10.1103/PhysRevA.102.033337](https://doi.org/10.1103/PhysRevA.102.033337).
- [9] C. Chen, G. Emperauger, G. Bornet, F. Caleca, B. Gély, M. Bintz, S. Chatterjee, V. Liu, D. Barredo, N. Y. Yao, T. Lahaye, F. Mezzacapo *et al.*, *Spectroscopy of elementary excitations from quench dynamics in a dipolar xy rydberg simulator*, doi:[10.48550/arXiv.2311.11726](https://doi.org/10.48550/arXiv.2311.11726) (2024).
- [10] S. Diehl, A. Micheli, A. Kantian, B. Kraus, H. P. Büchler and P. Zoller, *Quantum states and phases in driven open quantum systems with cold atoms*, Nature Physics **4**, 878 (2008), doi:[10.1038/nphys1073](https://doi.org/10.1038/nphys1073).
- [11] B. Kraus, H. P. Büchler, S. Diehl, A. Kantian, A. Micheli and P. Zoller, *Preparation of entangled states by quantum markov processes*, Phys. Rev. A **78**, 042307 (2008), doi:[10.1103/PhysRevA.78.042307](https://doi.org/10.1103/PhysRevA.78.042307).
- [12] F. Verstraete, M. M. Wolf and J. Ignacio Cirac, *Quantum computation and quantum-state engineering driven by dissipation*, Nature Physics **5**, 633 (2009), doi:[10.1038/nphys1342](https://doi.org/10.1038/nphys1342).
- [13] M. Esposito and P. Gaspard, *Exactly solvable model of quantum diffusion*, Journal of Statistical Physics **121** (2005), doi:[10.48550/arXiv.1212.1436](https://doi.org/10.48550/arXiv.1212.1436).
- [14] M. Esposito and P. Gaspard, *Emergence of diffusion in finite quantum systems*, Phys. Rev. B **71**, 214302 (2005), doi:[10.1103/PhysRevB.71.214302](https://doi.org/10.1103/PhysRevB.71.214302).
- [15] V. Eisler, *Crossover between ballistic and diffusive transport: the quantum exclusion process*, Journal of Statistical Mechanics: Theory and Experiment **2011**(06), P06007 (2011), doi:[10.1088/1742-5468/2011/06/P06007](https://doi.org/10.1088/1742-5468/2011/06/P06007).
- [16] J.-S. Bernier, R. Tan, L. Bonnes, C. Guo, D. Poletti and C. Kollath, *Light-cone and diffusive propagation of correlations in a many-body dissipative system*, Physical Review Letters **120**(2) (2018), doi:[10.1103/PhysRevLett.120.020401](https://doi.org/10.1103/PhysRevLett.120.020401).
- [17] X. Turkeshi and M. Schiró, *Diffusion and thermalization in a boundary-driven dephasing model*, Phys. Rev. B **104**, 144301 (2021), doi:[10.1103/PhysRevB.104.144301](https://doi.org/10.1103/PhysRevB.104.144301).
- [18] V. Alba and F. Carollo, *Spreading of correlations in markovian open quantum systems*, Physical Review B **103**(2) (2021), doi:[10.1103/PhysRevB.103.L020302](https://doi.org/10.1103/PhysRevB.103.L020302).
- [19] P. Grišins, B. Rauer, T. Langen, J. Schmiedmayer and I. E. Mazets, *Degenerate bose gases with uniform loss*, Phys. Rev. A **93**, 033634 (2016), doi:[10.1103/PhysRevA.93.033634](https://doi.org/10.1103/PhysRevA.93.033634).
- [20] B. Rauer, P. Grišins, I. E. Mazets, T. Schweigler, W. Rohringer, R. Geiger, T. Langen and J. Schmiedmayer, *Cooling of a one-dimensional bose gas*, Phys. Rev. Lett. **116**, 030402 (2016), doi:[10.1103/PhysRevLett.116.030402](https://doi.org/10.1103/PhysRevLett.116.030402).
- [21] N. Syassen, D. M. Bauer, M. Lettner, T. Volz, D. Dietze, J. J. García-Ripoll, J. I. Cirac, G. Rempe and S. Dürr, *Strong dissipation inhibits losses and induces correlations in cold molecular gases*, Science **320**(5881) (2008), doi:[10.1126/science.1155309](https://doi.org/10.1126/science.1155309).
- [22] B. Yan, S. A. Moses, B. Gadway, J. P. Covey, K. R. A. Hazzard, A. M. Rey, D. S. Jin and J. Ye, *Observation of dipolar spin-exchange interactions with lattice-confined polar molecules*, Nature **501** (2013), doi:[10.1038/nature12483](https://doi.org/10.1038/nature12483).
- [23] G. Barontini, R. Labouvie, F. Stubenrauch, A. Vogler, V. Guarrera and H. Ott, *Controlling the dynamics of an open many-body quantum system with localized dissipation*, Phys. Rev. Lett. **110**, 035302 (2013), doi:[10.1103/PhysRevLett.110.035302](https://doi.org/10.1103/PhysRevLett.110.035302).
- [24] V. Alba and F. Carollo, *Noninteracting fermionic systems with localized losses: Exact results in the hydrodynamic limit*, Physical Review B **105**(5) (2022), doi:[10.1103/PhysRevB.105.054303](https://doi.org/10.1103/PhysRevB.105.054303).
- [25] L. Rosso, D. Rossini, A. Biella and L. Mazza, *One-dimensional spin-1/2 fermionic gases with two-body losses: Weak dissipation and spin conservation*, Phys. Rev. A **104**, 053305 (2021), doi:[10.1103/PhysRevA.104.053305](https://doi.org/10.1103/PhysRevA.104.053305).
- [26] L. Rosso, A. Biella, J. De Nardis and L. Mazza, *Dynamical theory for one-dimensional fermions with strong two-body losses: Universal non-hermitian zeno physics and spin-charge separation*, Phys. Rev. A **107**, 013303 (2023), doi:[10.1103/PhysRevA.107.013303](https://doi.org/10.1103/PhysRevA.107.013303).

- [27] G. Mazza and M. Schirò, *Dissipative dynamics of a fermionic superfluid with two-body losses*, Phys. Rev. A **107**, L051301 (2023), doi:[10.1103/PhysRevA.107.L051301](https://doi.org/10.1103/PhysRevA.107.L051301).
- [28] R. Fazio, J. Keeling, L. Mazza and M. Schirò, *Many-body open quantum systems*, doi:[10.48550/arXiv.2409.10300](https://doi.org/10.48550/arXiv.2409.10300) (2024).
- [29] H.-P. Breuer and F. Petruccione, *The Theory of Open Quantum Systems*, Oxford University Press (2007).
- [30] Y. Ashida, Z. Gong and M. Ueda, *Non-hermitian physics*, Advances in Physics **69**(3), 249 (2020), doi:[10.1080/00018732.2021.1876991](https://doi.org/10.1080/00018732.2021.1876991).
- [31] A. J. Daley, *Quantum trajectories and open many-body quantum systems*, Advances in Physics **63**(2), 77 (2014), doi:[10.1080/00018732.2014.933502](https://doi.org/10.1080/00018732.2014.933502).
- [32] I. Bloch, J. Dalibard and S. Nascimbène, *Quantum simulations with ultracold quantum gases*, Nat. Phys.**8**(2), 267 (2012), doi:[10.1038/nphys2259](https://doi.org/10.1038/nphys2259).
- [33] C. Gross and I. Bloch, *Quantum simulations with ultracold atoms in optical lattices*, Science **357**(6355), 995 (2017), doi:[10.1126/science.aal3837](https://doi.org/10.1126/science.aal3837).
- [34] W. S. Bakr, A. Peng, M. E. Tai, R. Ma, J. Simon, J. I. Gillen, S. Fölling, L. Pollet and M. Greiner, *Probing the superfluid-to-mott insulator transition at the single-atom level*, Science **329**(5991), 547 (2010), doi:[10.1126/science.1192368](https://doi.org/10.1126/science.1192368).
- [35] D. Chen, M. White, C. Borries and B. DeMarco, *Quantum quench of an atomic mott insulator*, Phys. Rev. Lett. **106**, 235304 (2011), doi:[10.1103/PhysRevLett.106.235304](https://doi.org/10.1103/PhysRevLett.106.235304).
- [36] S. Trotzky, Y.-A. Chen, A. Flesch, I. P. McCulloch, U. Schollwöck, J. Eisert and I. Bloch, *Probing the relaxation towards equilibrium in an isolated strongly correlated one-dimensional Bose gas*, Nat. Phys.**8**, 325 (2012), doi:[10.1038/nphys2232](https://doi.org/10.1038/nphys2232).
- [37] M. Seclì, M. Capone and M. Schirò, *Steady-state quantum zeno effect of driven-dissipative bosons with dynamical mean-field theory*, Phys. Rev. A **106**, 013707 (2022), doi:[10.1103/PhysRevA.106.013707](https://doi.org/10.1103/PhysRevA.106.013707).
- [38] Z. Ren, D. Liu, E. Zhao, C. He, K. K. Pak, J. Li and G.-B. Jo, *Chiral control of quantum states in non-hermitian spin-orbit-coupled fermions*, Nature Physics **18** (2022), doi:[10.48550/arXiv.2106.04874](https://doi.org/10.48550/arXiv.2106.04874).
- [39] D. Eberz, A. Kell, M. Breyer and M. Köhl, *Cooling a strongly-interacting quantum gas by interaction modulation*, doi:[10.48550/arXiv.2410.10642](https://doi.org/10.48550/arXiv.2410.10642) (2024), [2410.10642](https://arxiv.org/abs/2410.10642).
- [40] Browaeys, A., Poupard, J., Robert, A., Nowak, S., Rooijackers, W., Arimondo, E., Marcassa, L., Boiron, D., Westbrook, C. I. and Aspect, A., *Two body loss rate in a magneto-optical trap of metastable He*, Eur. Phys. J. D **8**(2) (2000), doi:[10.1007/s100530050027](https://doi.org/10.1007/s100530050027).
- [41] L. Franchi, L. F. Livi, G. Cappellini, G. Binella, M. Inguscio, J. Catani and L. Fallani, *State-dependent interactions in ultracold ^{174}Yb probed by optical clock spectroscopy*, New Journal of Physics **19**(10), 103037 (2017), doi:[10.1088/1367-2630/aa8fb4](https://doi.org/10.1088/1367-2630/aa8fb4).
- [42] T. Tomita, S. Nakajima, I. Danshita, Y. Takasu and Y. Takahashi, *Observation of the mott insulator to superfluid crossover of a driven-dissipative bose-hubbard system*, Science Advances **3**(12), e1701513 (2017), doi:[10.1126/sciadv.1701513](https://doi.org/10.1126/sciadv.1701513).
- [43] J. Weiner, V. S. Bagnato, S. Zilio and P. S. Julienne, *Experiments and theory in cold and ultracold collisions*, Rev. Mod. Phys. **71**, 1 (1999), doi:[10.1103/RevModPhys.71.1](https://doi.org/10.1103/RevModPhys.71.1).
- [44] B. Raphaël, B. A. Manel, G. Alexis and B. Jérôme, *Anomalous decay of coherence in a dissipative many-body system*, Nature Physics **16** (2020), doi:[10.1038/s41567-019-0678-2](https://doi.org/10.1038/s41567-019-0678-2).
- [45] M. Greiner, O. Mandel, T. W. Hänsch and I. Bloch, *Collapse and revival of the matter wave field of a Bose-Einstein condensate*, Nature (London)**419**, 51 (2002), doi:[10.1038/nature00968](https://doi.org/10.1038/nature00968).
- [46] T. Langen, R. Geiger, M. Kuhnert, B. Rauer and J. Schmiedmayer, *Local emergence of thermal correlations in an isolated quantum many-body system*, Nat. Phys.**9**, 640 (2013), doi:[10.1038/nphys2739](https://doi.org/10.1038/nphys2739).

- [47] R. Geiger, T. Langen, I. E. Mazets and J. Schmiedmayer, *Local relaxation and light-cone-like propagation of correlations in a trapped one-dimensional Bose gas*, *New J. Phys.* **16**, 053034 (2014), doi:[10.1088/1367-2630/16/5/053034](https://doi.org/10.1088/1367-2630/16/5/053034).
- [48] P. Calabrese and J. Cardy, *Time dependence of correlation functions following a quantum quench*, *Phys. Rev. Lett.* **96**, 136801 (2006), doi:[10.1103/PhysRevLett.96.136801](https://doi.org/10.1103/PhysRevLett.96.136801).
- [49] P. Barmettler, D. Poletti, M. Cheneau and C. Kollath, *Propagation front of correlations in an interacting bose gas*, *Physical Review A* **85**(5) (2012), doi:[10.1103/PhysRevA.85.053625](https://doi.org/10.1103/PhysRevA.85.053625).
- [50] C. Kollath, A. M. Läuchli and E. Altman, *Quench dynamics and nonequilibrium phase diagram of the Bose-Hubbard model*, *Phys. Rev. Lett.* **98**, 180601 (2007), doi:[10.1103/PhysRevLett.98.180601](https://doi.org/10.1103/PhysRevLett.98.180601).
- [51] M. Moeckel and S. Kehrein, *Interaction quench in the Hubbard model*, *Phys. Rev. Lett.* **100**, 175702 (2008), doi:[10.1103/PhysRevLett.100.175702](https://doi.org/10.1103/PhysRevLett.100.175702).
- [52] S. R. Manmana, S. Wessel, R. M. Noack and A. Muramatsu, *Time evolution of correlations in strongly interacting fermions after a quantum quench*, *Phys. Rev. B* **79**, 155104 (2009), doi:[10.1103/PhysRevB.79.155104](https://doi.org/10.1103/PhysRevB.79.155104).
- [53] G. Roux, *Finite-size effects in global quantum quenches: Examples from free bosons in an harmonic trap and the one-dimensional bose-hubbard model*, *Phys. Rev. A* **81**, 053604 (2010), doi:[10.1103/PhysRevA.81.053604](https://doi.org/10.1103/PhysRevA.81.053604).
- [54] P. Navez and R. Schützhold, *Emergence of coherence in the Mott insulator-superfluid quench of the Bose-Hubbard model*, *Phys. Rev. A* **82**, 063603 (2010), doi:[10.1103/PhysRevA.82.063603](https://doi.org/10.1103/PhysRevA.82.063603).
- [55] G. Carleo, F. Becca, L. Sanchez-Palencia, S. Sorella and M. Fabrizio, *Light-cone effect and supersonic correlations in one- and two-dimensional bosonic superfluids*, *Phys. Rev. A* **89**, 031602(R) (2014), doi:[10.1103/PhysRevA.89.031602](https://doi.org/10.1103/PhysRevA.89.031602).
- [56] K. V. Krutitsky, P. Navez, F. Queisser and R. Schützhold, *Propagation of quantum correlations after a quench in the mott-insulator regime of the bose-hubbard model*, *EPJ Quantum Technology* **1**(1) (2014), doi:[10.1140/epjqt12](https://doi.org/10.1140/epjqt12).
- [57] L. Cevolani, J. Despres, G. Carleo, L. Tagliacozzo and L. Sanchez-Palencia, *Universal scaling laws for correlation spreading in quantum systems with short- and long-range interactions*, *Phys. Rev. B* **98**, 024302 (2018), doi:[10.1103/PhysRevB.98.024302](https://doi.org/10.1103/PhysRevB.98.024302).
- [58] J. Despres, L. Villa and L. Sanchez-Palencia, *Twofold correlation spreading in a strongly correlated lattice bose gas*, *Scientific Reports* **9**(1) (2019), doi:[10.1038/s41598-019-40679-3](https://doi.org/10.1038/s41598-019-40679-3).
- [59] J. Despres, L. Mazza and M. Schirò, *Dynamics of the bose-hubbard model induced by on-site or long-range two-body losses*, in preparation (2024).
- [60] C. Wang, C. Liu and Z.-Y. Shi, *Complex contact interaction for systems with short-range two-body losses*, *Phys. Rev. Lett.* **129**, 203401 (2022), doi:[10.1103/PhysRevLett.129.203401](https://doi.org/10.1103/PhysRevLett.129.203401).
- [61] C. Liu, Z. Shi and C. Wang, *Weakly interacting Bose gas with two-body losses*, *SciPost Phys.* **16**, 116 (2024), doi:[10.21468/SciPostPhys.16.5.116](https://doi.org/10.21468/SciPostPhys.16.5.116).
- [62] S. Sachdev, *Quantum Phase Transitions*, Cambridge University Press, Cambridge, UK (2001).
- [63] M. A. Cazalilla, R. Citro, T. Giamarchi, E. Orignac and M. Rigol, *One dimensional bosons: From condensed matter systems to ultracold gases*, *Rev. Mod. Phys.* **83**, 1405 (2011), doi:[10.1103/RevModPhys.83.1405](https://doi.org/10.1103/RevModPhys.83.1405).
- [64] T. D. Kühner, S. R. White and H. Monien, *One-dimensional bose-hubbard model with nearest-neighbor interaction*, *Physical Review B* **61**(18), 12474 (2000), doi:[10.1103/PhysRevB.61.12474](https://doi.org/10.1103/PhysRevB.61.12474).
- [65] V. Kashurnikov and B. Svistunov, *Exact diagonalization plus renormalization-group theory: Accurate method for a one-dimensional superfluid-insulator-transition study*, *Phys. Rev. B* **53**, 11776 (1996), doi:[10.1103/PhysRevB.53.11776](https://doi.org/10.1103/PhysRevB.53.11776).
- [66] S. Ejima, H. Fehske and F. Gebhard, *Dynamic properties of the one-dimensional bose-hubbard model*, *Europhys. Lett.* **93**, 30002 (2011), doi:[10.1209/0295-5075/93/30002](https://doi.org/10.1209/0295-5075/93/30002).
- [67] S. Rombouts, K. Van Houcke and L. Pollet, *Loop updates for quantum Monte Carlo simulations in the canonical ensemble*, *Phys. Rev. Lett.* **96**, 180603 (2006), doi:[10.1103/PhysRevLett.96.180603](https://doi.org/10.1103/PhysRevLett.96.180603).

- [68] J. Despres, *Correlation spreading in quantum lattice models with variable-range interactions*, doi:[10.48550/arXiv.2410.03125](https://doi.org/10.48550/arXiv.2410.03125) (2024).
- [69] G. Roux, A. Minguzzi and T. Roscilde, *Dynamic structure factor of one-dimensional lattice bosons in a disordered potential: a spectral fingerprint of the bose-glass phase*, *New Journal of Physics* **15**(5), 055003 (2013), doi:[10.1088/1367-2630/15/5/055003](https://doi.org/10.1088/1367-2630/15/5/055003).
- [70] L. Villa, S. J. Thomson and L. Sanchez-Palencia, *Finding the phase diagram of strongly correlated disordered bosons using quantum quenches*, *Phys. Rev. A* **104**, 023323 (2021), doi:[10.1103/PhysRevA.104.023323](https://doi.org/10.1103/PhysRevA.104.023323).
- [71] L. Villa, S. J. Thomson and L. Sanchez-Palencia, *Quench spectroscopy of a disordered quantum system*, *Phys. Rev. A* **104**, L021301 (2021), doi:[10.1103/PhysRevA.104.L021301](https://doi.org/10.1103/PhysRevA.104.L021301).
- [72] J. T. Stewart, J. P. Gaebler and D. S. Jin, *Using photoemission spectroscopy to probe a strongly interacting Fermi gas*, *Nature (London)* **454**(7205), 744 (2008), doi:[10.1038/nature07172](https://doi.org/10.1038/nature07172).
- [73] A. M. Rey, P. B. Blakie, G. Pupillo, C. J. Williams and C. W. Clark, *Bragg spectroscopy of ultracold atoms loaded in an optical lattice*, *Phys. Rev. A* **72**, 023407 (2005), doi:[10.1103/PhysRevA.72.023407](https://doi.org/10.1103/PhysRevA.72.023407).
- [74] J. Despres, L. Mazza and M. Schirò, *Breakdown of linear spin-wave theory in a non-hermitian quantum spin chain*, *Phys. Rev. B* **110**, 094304 (2024), doi:[10.1103/PhysRevB.110.094304](https://doi.org/10.1103/PhysRevB.110.094304).